Journal of Pharmaceutical and Biomedical Analysis 165 (2019) 207–212

Contents lists available at ScienceDirect

Journal of Pharmaceutical and Biomedical Analysis

journal homepage: www.elsevier.com/locate/jpba

A novel experimental approach for liver analysis in rats exposed to Bisphenol A by means of LC-mass spectrometry and infrared spectroscopy

Sonia Errico[a], Marianna Portaccio[a,*], Carla Nicolucci[a], Rosaria Meccariello[b], Rosanna Chianese[a], Marika Scafuro[a], Maria Lepore[a], Nadia Diano[a]

[a] Department of Experimental Medicine, University of Campania "L. Vanvitelli", Via S. M. di Costantinopoli, 16, 80138, Naples, Italy
[b] Department of Movement Sciences and Wellbeing, University of Naples "Parthenope", Via Medina, 40, 80133, Naples, Italy

ARTICLE INFO

Article history:
Received 11 September 2018
Received in revised form 7 December 2018
Accepted 8 December 2018
Available online 10 December 2018

Keywords:
Mass spectrometry
Infrared spectroscopy
Bisphenol A exposure
Rat liver
Metabolic disturbance

ABSTRACT

An innovative complementary approach using a liquid chromatographic-mass spectrometer method and infrared spectroscopy is proposed for measuring internal biological exposure to dangerous chemical contaminants and for monitoring biochemical changes in target organs. The proposed methodologies were validated and applied in the case of rats exposed to low-doses of Bisphenol A (BPA). A liquid chromatographic method coupled to a tandem mass spectrometer was used in order to measure BPA concentration in rat livers. BPA was detected at different levels in all liver samples from BPA-treated rats, although the exposure dose was the same in all treated animals, and also from control rats, highlighting the difficulties in eliminating external uncontrolled exposure and the need for internal biological monitoring. Fourier Transform Infrared analysis was applied to detect structural changes occurring in several molecules (lipids, proteins, carbohydrates and nucleic acids) as well as the presence of specific metabolic processes. The spectroscopic analyses clearly demonstrated a different lipid composition more than an evident lipid accumulation and a glycogen accumulation decrease, revealing a metabolic disturbance in livers with a normal histological aspect.

These results demonstrated the potential of an integrated approach based on mass spectrometry and infrared spectroscopy to evaluate at an early stage the hepatotoxic effect of BPA exposure in an animal model. This approach can be usefully exploited in all the investigations aimed to provide better information concerning the interrelationships between contaminant exposure, dose, and health effects.

1. Introduction

Several instrumental and analytical methodologies have been developed for assessing exposure to chemicals, which are reported in human health studies. In the scientific community, the exposure to environmental pollutants is considered a source of health risk [1]. It is now well established that diseases are due to complex interactions between genetic and environmental factors, such as infectious agents, lifestyle, nutrition, stress and also chemical pollutants [2,3].

To investigate the link between environmental pollution and health consequences, biomonitoring must be performed through highly sensitive methodologies and exposure assessment must be based on measurements of pollutant concentrations in biological fluids and/or in target tissues [4,5]. These data are crucial for the development of interpretative models which are able to correlate the bioaccumulation of these chemical pollutants with physiological alterations in organisms that are exposed to them [4].

It is important to emphasise that in studies based on an animal model, the external exposure dose does not correspond to the internal biological dose or rather the biologically effective dose. Differences in internal exposures corresponding to equivalent external doses, coupled with variations in individual susceptibility, introduce a large measure of uncertainty in health risk assessment [4]. Thus, there is an acute need for methods that provide better information concerning the interrelationships between exposure, dose, and health effects.

For this reason, we propose an integrated approach that allows us to derive measurements of internal biological exposure and to measure early changes in biological processes at the molecular level.

* Corresponding author.
E-mail address: marianna.portaccio@unicampania.it (M. Portaccio).

https://doi.org/10.1016/j.jpba.2018.12.011
0731-7085/

Recently, we have focused our research activity on investigating the relationship between Bisphenol A (BPA), an endocrine-disrupting chemical, and metabolic disease occurrence. BPA is involved in the modulation of genes related to lipid synthesis, increased body weight, lipid accumulation and insulin secretion [6,7]. In particular, in the liver, a target organ for accumulation, decomposition and biological transmission of environmental contaminants, BPA may influence an excessive *de novo* fatty acid synthesis, and consequently, contribute to the pathogenesis of hepatic steatosis and steatohepatitis (NASH) [8].

This study aims at validating complementary methodologies in order to characterize the liver of rats exposed to BPA. In order to investigate an association between BPA exposure and liver health status, the amount of BPA in the liver and pollutant-induced changes in the liver macromolecular structure must be analyzed. Nowadays, many techniques are available for BPA detection, such as amperometric, chemical, electrochemical, SERS- and grapheme oxide – based sensors [9,10, and references therein]. ELISA assays are also often considered but they are not adequate for the determination of BPA in biological samples due to the presence of structurally and biologically similar molecules (endogenous hormones) that influence their specificity [11] Among all of the analytical techniques available, mass spectrometry, specifically coupled with liquid chromatography, is considered the most accurate and precise method for measuring low levels of BPA and other environmental chemicals in biological samples. Our previous experience [12,13] has helped us to set up the methodology described in this study.

In addition, Fourier Transform Infrared (FT-IR) analysis is considered one of the most accurate techniques to elucidate the molecular and structural changes in response to various treatments. Moreover, it can be considered a rapid, high-throughput, noninvasive and very sensitive technology that can reveal very small alterations in bonds within functional groups of molecules [14]. Many reports have characterized hepatic tissues using infrared spectroscopy [15] but only a few authors [16] have utilized this technology to study the biological effects due to chemical pollutant exposures that can predict adverse outcomes.

2. Materials and methods

2.1. Chemicals and reference materials

HPLC grade reagents, including ultrapure water, acetonitrile (ACN) and methanol (MeOH) were purchased from Romil (ROMIL Ltd, UK). BPA (native and d_6) and reagents were purchased from Sigma Aldrich (Sigma-Aldrich, Milano, Italy). MIP cartridges were AFFINIMIP® solid-phase extraction (SPE) BPA in glass tube and were purchased from Polyntell (Polyntell SA, Paris, France).

Stock standard solutions and quality control samples (QCs) at three BPA levels (1, 10, 50 ng) were prepared as reported in Nicolucci et al. [13]. The liver from two rats was chosen as reference samples for determination of accuracy and recovery, intraday and interday precision.

2.2. Animals and BPA exposure protocol

Wistar rats (Harlan Laboratories) were kept under standard humidity and temperature conditions with a 12:12 light/dark cycle (lights on at 07:00 am) and free access to standard fresh food and water, in accordance according with the rules of the European Union Guide for the Care and Use of Laboratory Animals.

BPA exposure was performed as recently reported [17]. In brief, after the coupling period, female rats were exposed to BPA (0.1 mg/L in drinking water in glass bottles, n = 2) or to vehicle (ethanol at 0.1 mL/L in drinking water, n = 3) from gestation to lactation period. At weaning, newborns received the same treatment of the mother *via* drinking water. A daily dose of 10 μg/kg bw was calculated based on daily drinking consumption. The male newborns (n = 2–3/dam, randomly chosen) were sacrificed at 60 postnatal dies following deep anaesthesia by an overdose of Tanax (0.1 mL intrapulmonary) to collect liver. Tissues were cut and partially stored at −80 °C or fixed in Bouin's fluid for histological analysis. Experimental protocols were approved by the local Ethical Committees and by the Italian Ministry of Education, University and Research (45/2014-PR 17/11/2014).

2.3. Sample preparation and instrumental analysis

The liquid-liquid extraction with MeOH coupled to a solid phase extraction by AFFINIMIP® SPE columns was used to extract BPA from liver, according to the procedure previously described [12]. The samples were then analysed by a Dionex UltiMate 3000 HPLC system (Thermo Fisher Scientific Inc, Italy) coupled to a triple quadrupole instrument (API 2000; AB Sciex, Germany) equipped with a Turbolon electrospray source. The chromatographic separation and instrumental parameters were reported in Nicolucci et al. [13].

The analyte identification was based on multiple reaction monitoring (MRM). The target compounds were specifically identified not only by the retention time but also by monitoring the following ion transitions: *m/z* 227.1• *m/z* 212.1 (quantifier) and *m/z* 227.1• *m/z* 133.2 (qualifier) for BPA; *m/z* 233.1• *m/z* 215.0 (quantifier) and *m/z* 233.1• *m/z* 138.2 (qualifier) for d_6-BPA.

2.4. FTIR spectroscopy

Rat liver was examined by Fourier Transform Infrared spectroscopy (FTIR) to identify possible variations on the functional groups of organic molecules following exposure to BPA. FTIR spectra were obtained using a Perkin Elmer Spectrum One spectrometer in a transmission geometry using KBr pellets. Initially, 0,1 g of a liver sample was mixed with 5 mL water and sonicated on ice for 5 min by using a Soniprep 150 Plus Utrasonic Disgregator. The homogenate was stored at −20 °C for 24 h. After this, the sample was lyophilized (24 h), using a Lio-5P Freeze Dryer. KBr pellets were prepared by mixing a small quantity of liver powder with KBr (at the ratio of 1/100) [18]. For every sample two KBr pellets were prepared. All spectra were obtained using 64 scans in the range from 4000 to 450 cm^{-1} with a 4 cm^{-1} spectral resolution. Each measurement was performed in triplicate. The spectra were preliminarily analyzed using the application routines provided by the software package ("Spectrum" Perkin Elmer Inc., Hopkinton, MA, USA) controlling the whole data acquisition system.

The use of a univariate analysis similar to the one described in Ref. [19] allowed us to use average spectra for the discussion reported in paragraph 3.6.

2.5. Tissue section

Liver samples were fixed in Bouin's solution and processed for paraffin embedding following standard procedures. Subsequently, sections (5 μm) were stained with hematoxylin and eosin and they were observed under a light microscope (CTR500, Leica) to assess the morphology of hepatic tissues. Images were obtained by using a high-resolution digital camera (DC300 F; Leica).

2.6. Statistical analysis

Data were shown as the mean ± standard deviation (SD). Statistically significant differences were assessed by one-way ANOVA

Table 1
Mean percentage recoveries, matrix effect, precision in spiked livers.

BPA added (ng)	Matrix effect (%)	Recovery (%)	Precision (%RDS)		Accuracy (%)
			Intraday	Interday	
1	71.2	98.6	14.1	17.9	102.1
10	88.2	87.5	15.0	16.4	92.3
50	85.4	82.9	12.9	15.1	82.2

followed by an unpaired, two-tailed independent sample T-test. A P-value less than 0.05 was considered statistically significant. Statistical analysis was done by using GraphPad Prism 5.0 H statistical software (GraphPad Software Inc., La Jolla, CA).

3. Results and discussion

3.1. Validation of BPA analysis in rat liver tissues

The analytical method, previously published [12,13], was set-up for rat liver and then validated according to FDA Guidance for Industry [20]. The calibration curves for BPA detection were obtained by performing a linear regression analysis on peak area ratios of BPA and IS against BPA standard concentrations ranging from 0.1 to 200 ng/mL, containing internal standard at 100 ng/mL. Good linearity was obtained with the correlation coefficient (R^2, weighting factor *1/x*) of no less than 0.994. The limit of detection (LOD) of the detectors is 0.01 ng/mL. The limit of quantification (LOQ) of the HPLC method is 0.1 ng/mL.

In the chromatograms (not shown), a lower baseline noise was observed, and no interfering peaks from the matrix were detected, proving effective sample clean-up. Ion suppression in the analyte responses was observed and a matrix effect for each analyte in QCs was calculated in a range 71.2–88.2%. Since isotope-labeled internal standard (IS) was used in this study and the results showed the same degree of ion suppression in internal standard, the quantification based on the analyte/IS response ratios allowed us to correct the matrix effect.

The analyte recovery of extraction procedure was evaluated by spiking different levels of standard analyte and internal standard to samples at three levels in 5 replicates. The results are reported in Table 1. The effective mean recoveries, without considering compensation due to the labeled IS, ranged from 82.9 to 98.6%.

The interday precision was evaluated by considering five spiked samples for every concentration level, on three consecutive working days (n = 15). The intraday precision was expressed as RSD and was found to be equal to or lower than 15%, whereas interday precision was at maximum 18% (Table 1). The accuracy, determined by comparing the mean result for five analyses to the nominal concentration value, was between 82.1 and 102.1% at all concentration levels.

For each set of samples, to capture possible environmental contamination and avoid cross contaminations, procedural blanks were processed and handled similarly to the actual samples. If traces of BPA were detected in method blanks, the values were subtracted from sample concentrations. All the results were very satisfactory, indicating that both the extraction procedure and analytical method are highly reliable.

3.2. Concentrations of BPA in rat liver

The previously validated method was applied to analyze real samples of rats exposed to BPA. By measuring the concentrations of BPA in the liver, we verified that BPA exposure had occurred. It is important to note that the liver is a target tissue, the primary organ responsible for BPA metabolism in humans and animals [21]. Therefore, it can be extensively exposed to BPA and be susceptible to lower doses more than other organs [22].

BPA was detected above the detection limit in all liver samples from BPA-treated and control rats, highlighting the difficulties in eliminating external and uncontrolled exposure. Environmental sources of this chemical are known and it is practically impossible to totally eliminate external contaminations. When low levels of exposure are used in the studies, contamination effects can obscure the true exposures and negatively influence the estimation of potential adverse health effects. A part of the scientific community asserts that the studies in rodents have provided inconsistent data regarding its estrogenic activity and toxicity, due to the fact that BPA is found in a lot of equipment used during laboratory experiments, thereby contributing to unwanted exposure [23,24]. Therefore, it is of critical importance to develop and validate the analytical methods which are able to measure the real values of bioaccumulation in target organ/tissue.

The values of BPA concentration in the liver expressed per g of tissue, ranged from 0.52 to 19.61 μg g^{-1}. Nevertheless, the mean value of concentration in the liver of BPA-treated rats was about 8 times higher than the corresponding value in control rats (8.07 ± 2.60 μg g^{-1} vs 1.02 ± 0.25 μg g^{-1}, $p = 0.0041$). Moreover, BPA-treated rats showed a different hepatic bioaccumulation although the exposure dose was the same in all treated animals, confirming the need to perform internal biological monitoring. In particular, BPA-treated livers were classified into two groups: high BPA level and medium BPA level (Table 2). In contrast, the livers from control rats belonged to a low BPA level class.

Table 2
Classification of liver samples for FTIR spectroscopy measurements according to BPA concentration determination by LC/ESI-MS/MS analysis.

Class name	Recovered BPA concentration (μg/g)
Low BPA level	0. 52–1.32
Medium BPA level	2.41–4.85
High BPA level	8.44–19.61

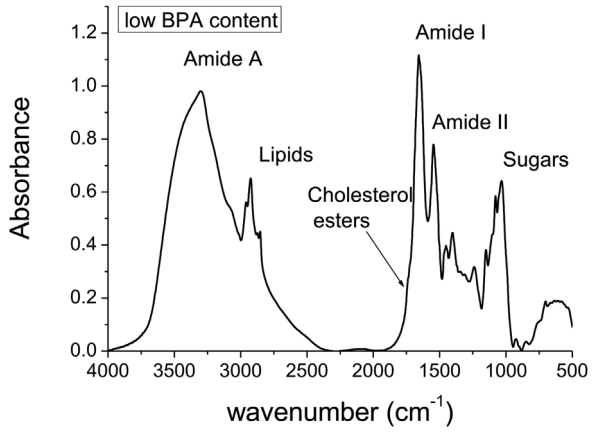

Fig. 1. Representative infrared spectrum for liver samples with low BPA level. The spectral range due to the main contributions from proteins, lipids and sugars are indicated.

3.3. FTIR spectroscopy results

The results obtained by FTIR spectroscopy on liver samples were presented using the three different classes as reported in Table 2. In Fig. 1, a representative infrared spectrum of rat liver samples with a low BPA level is reported. In the spectrum, the typical bands assigned to functional groups of macromolecules present in the liver tissue can be seen [18,25,26]. A large band was present at 3302 cm^{-1} that was mainly ascribed to the N—H

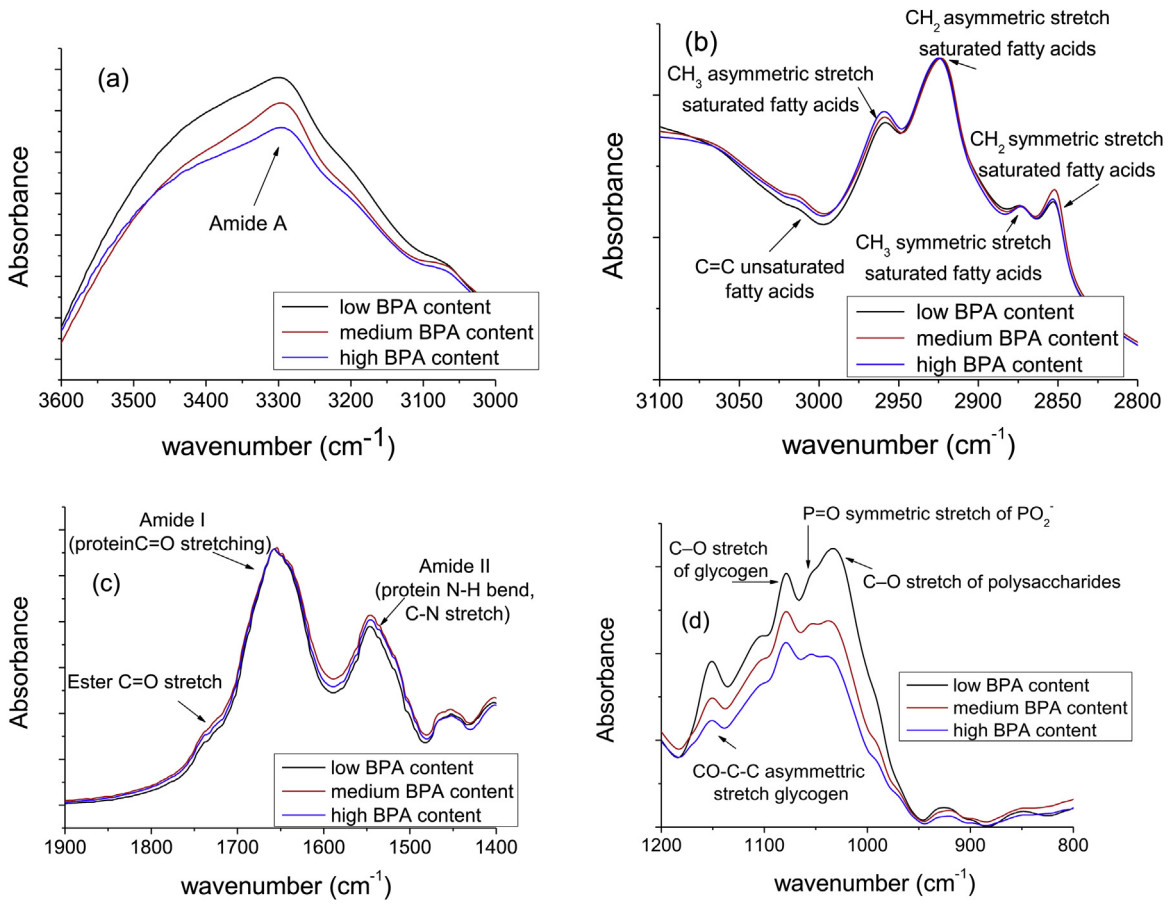

Fig. 2. The infrared spectra of livers treated with low, medium and high BPA levels (**a**) in the 3600 – 3030 cm^{-1} region (the spectra were normalized with respect to the CH_2 asymmetric stretch mode, which is observed at 2927 cm^{-1}); (**b**) in the 3100–2800 cm^{-1} region (the spectra were normalized with respect to the CH_2 asymmetric stretch mode, which is observed at 2927 cm^{-1}); (**c**) The infrared spectra of livers treated with low, medium and high BPA levels in the 1800–800 cm^{-1} region (the spectra were normalized with respect to the amide I band, which is observed at 1658 cm^{-1}); (**d**) The infrared spectra of livers treated with low, medium and high BPA levels in the 1200–800 cm^{-1} region (the spectra were normalized with respect to the amide I band, shown in panel c).

stretching (Amide I) of proteins with few contributions from O—H stretching of polysaccharides and intermolecular H bonding. In the 3100–2800 cm^{-1} region, it was also possible to recognize the contribution of functional groups of lipids, due specifically to C=C stretching at 3060 cm^{-1}, CH_3 asymmetric stretching at 2959 cm^{-1}, CH_2 asymmetric stretching at 2927 cm^{-1} and CH_3 symmetric stretching at 2876 cm^{-1}. A faint contribution to ester C=O stretching was also present near 1740 cm^{-1}. In the 1660-1550 cm^{-1} region the most relevant contribution of the functional groups of proteins was clearly present with Amide I (C=O stretching) and Amide II (N—H bending) bands at 1658 and 1552 cm^{-1}, respectively. The bands given to the functional groups of polysaccharides were present in the 1150-950 cm^{-1} region. In particular, the peak at 1150 cm^{-1} was mainly attributed to the CO—C—C asymmetric stretching of glycogen. In this region, it was also possible to identify a contribution at 1080 cm^{-1} ascribed to PO_{-2} symmetric stretching of nucleic acids and at 1040 cm^{-1} due to C–O stretching of polysaccharides. In addition, at 1452, 1400 and 1244 cm^{-1} the contributions due to CH_2 bending, COO- symmetric stretching of fatty acids and PO_{-2} asymmetric stretching were, respectively, present. As is well known [25,26], the greatest variations in the absorbance values in the IR spectra of liver samples were expected in the lipid region around 3000–2800 cm^{-1} and in the ester region around 1760–1710 cm^{-1}. Changes were also expected in the wave number domain 1200-950 cm^{-1} corresponding in part to polysaccharide contribution. To perform an accurate analysis and to highlight significant variations, we analyzed in greater detail the single spectral regions using appropriate normalizations and calculating, in some cases, the ratio between the intensities of certain characteristic peaks. In Fig. 2a, the infrared spectra of liver samples with low, medium and high BPA levels in the 3600–3030 cm^{-1} region are reported. The spectra were normalized with respect to the CH_2 asymmetric stretch mode, observed at 2927 cm^{-1}. A significant decrease was observed in Fig. 2a, due probably to reduced contribution of glycogen O—H absorbance as also reported by Severcan et al. [18] and Melin et al. [27]. This observation was strongly supported by the variation of the 1040 cm^{-1} contribution, assigned mainly to the C—O stretching vibrations in polysaccharides. This band was almost lost in the spectrum of the liver with a higher BPA level (see Fig. 2d).

In Fig. 2b, the 3100-2800 cm^{-1} region is reported for the three different liver classes. The spectra were normalized with respect to the CH_2 asymmetric stretch mode (2927 cm^{-1}). In this Figure, in addition to the contributions already outlined in Fig. 1, it was possible to notice two other structures located at 3015 and 2853 cm^{-1}. The intensity of the contribution at 3015 cm^{-1} (assigned to C=C unsaturated fatty acids) slightly increased indicating an increase in the unsaturated lipids in livers with higher BPA levels. This becomes evident by calculating the intensities ratio of this contribution (3015 cm^{-1}) to the CH_2 symmetric stretch saturated fatty acid peak to CH_3 symmetric stretch saturated fatty acid (2876 cm^{-1}) (see Fig. 3). In Fig. 2b, the contribution at 2853 cm^{-1} (assigned to CH_2 symmetric stretching of saturated fatty acid) also increased slightly. These data clearly demonstrated three clusters of samples

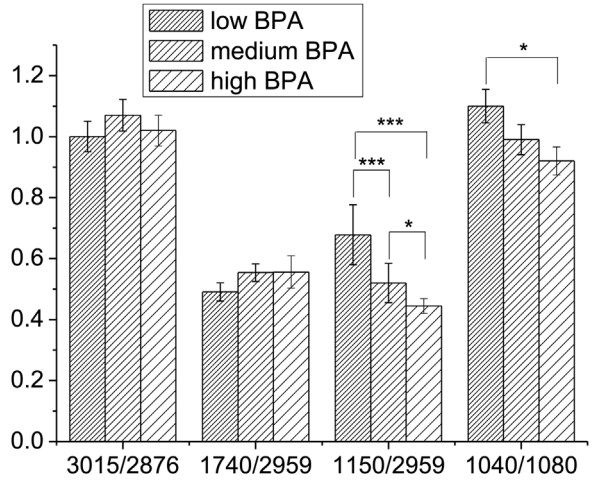

Fig. 3. Comparison of the mean values of saturated lipids, ester and glycogen contents for liver samples treated with low, medium and high BPA doses obtained by evaluating ratio of selected bands. The numerical values are expressed as the mean ± standard deviation evaluated by considering selected peak intensity values in the spectra acquired for each examined samples at different BPA dose. The asterisks indicate that a significant difference between intensity ratio occurred at $^{***}p < 0.001$; $^{**}p < 0.01$; $^{*}p < 0.05$.

due more to a different lipid composition than to an evident lipid accumulation. An increase in the $-CH_2$ functional groups suggested an increase of saturated fatty acids with longer carbon chains, such as palmitic acid (C16) and stearic acid (C18). The accumulation of fatty acids with elongated carbon chains may have promoted the biosynthesis, involving desaturase enzymes, first to monounsaturated fatty acids and then to polyunsaturated fatty acids [28]. This process was started in the livers with higher BPA level as demonstrated by the significant peak at 3015 cm^{-1} relative to C=C unsaturated fatty acids. In addition, the lower stability of the latter ones due to methylene groups between two double bonds, may have actived the radical process by the ROS with consequent oxidative degradation. Subsequently, an accumulation of unsaturated fatty acids linked to higher BPA levels might have exposed the liver to an insult by ROS, with consequent oxidative damage.

In Fig. 2c, the protein spectral region of the three liver classes is reported. In this case, the spectra were normalized with respect to the Amide I band at 1658 cm^{-1}. In all the spectra, the contributions of Amide I and Amide II were found to be very similar. The former one may give clear indications of changes in the secondary structure of proteins. In particular, the Amide I band may be affected by a wave number shift indicating an oxidative process for proteins [29]. In the present case, no similar shifts were obtained indicating that no oxidative process for the proteins in all the different examined samples was present. The absence of significant changes was also confirmed when the intensity ratio of Amide II to Amide I was calculated.

Regarding the contribution at 1740 cm^{-1} (see Fig. 2c) related to the functional group of esters (C=O), the livers with higher BPA levels exhibited barely detectable intensities. An increase of esters in the livers with higher BPA levels were found (see Fig. 3) only from the ratio of the intensity of this peak to the intensity of CH_3 asymmetric stretch saturated fatty acids (2959 cm^{-1}). This increase emphasizes an esterification of fatty acids with a consequent initial accumulation of triglycerides, i.e. an early stage of steatosis [30].

In Fig. 2d, the spectral region, normalized to Amide I peak, related to polysaccharides contribution is reported. There was a general intensity decrease for the rat liver samples with higher BPA levels. In particular, the decrease of 1150 cm^{-1} contribution related to glycogen was particularly significant. This decrease was also confirmed when the ratio between glycogen (1150 cm^{-1}) and CH_3 asymmetric stretch of saturated fatty acid (2959 cm^{-1}) peaks was calculated (see Fig. 3). This significant decrease for increasing BPA levels demonstrated a decrease in the glycogen levels, index of insulin resistance. In fact, in this state, the endogenous glucose suppression, no longer converted into glycogen by insulin action, is eliminated. Glucose, in high blood concentration (hyperglycaemia) and in the presence of high concentrations of insulin (hyperinsulinemia), promotes the synthesis of fatty acids by *de novo* lipogenesis with consequent triglyceride accumulation. This suggested that a better discrimination of liver classes was obtained based on sugar content rather than that based on lipids. In fact, Peng et al. [26] demonstrated that IR microspectroscopy enabled the discrimination of liver steatosis grades based also on their metabolic changes in sugars.

In addition, the ratio of absorbance at 1040 cm^{-1} (the C—O stretching vibration) to 1080 cm^{-1} (the phosphate symmetric stretching vibration) had a smaller value when the BPA level increased (see Fig. 3) indicating an increase in the content of nucleic acids in tissues [18].

IR spectroscopy allowed us to provide a biochemical characterization of rat livers highlighting the BPA-induced changes occurring in the hepatic tissue. The livers with higher BPA levels presented a different lipid composition and a glycogen accumulation decrease, indicating a metabolic disturbance preceding steatosis.

3.4. Morphological analyzes of rat liver tissues

To confirm the results of spectroscopic analyzes, in Fig. 4 histological features are shown. No significant alterations resulted in hepatic tissue from animals with low, medium or high BPA levels. The images did not clearly show the presence of lipid droplets. This confirmed that the rats exposed to BPA did not have a steatotic liver but probably they developed an insulin resistance.

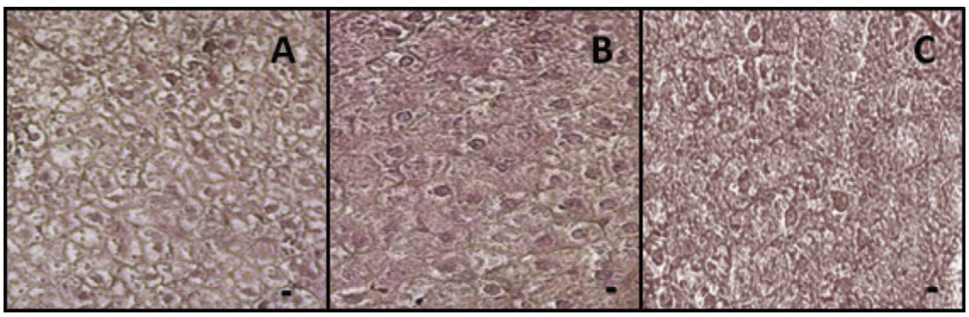

Fig. 4. Histological analysis of rat liver after staining with standard hematoxylin-eosin. Low (A), medium (B) and high (C) BPA levels. Scale bars = 20 μm.

4. Conclusions

The high sensitivity of a triple quadrupole LC/ESI-MS/MS method allowed us to demonstrate that BPA-treated rats showed a different hepatic bioaccumulation although the exposure dose was the same in all treated animals, confirming the need to perform internal biological monitoring.

In addition, FT-IR spectroscopy proved able to reveal important BPA-induced changes in not yet steatotic livers, with a normal histological aspect. We therefore note that the spectroscopic approach is a suitable method to reveal metabolic disturbance at an early stage.

Acknowledgments

This work was supported by University of Naples "L. Vanvitelli" (Italy) under the project "Ricerca Scientifica di Dipartimento" (2017) and by research fundings from the University of Naples Parthenope to Rosaria Meccariello.

References

[1] M. Kolossa-Gehringa, U. Fiddickea, G. Leng, J. Angerer, B. Wolz, New human biomonitoring methods for chemicals of concern—the German approach to enhance relevance, Int. J. Hyg. Environ. Health 220 (2017) 103–112.
[2] A. Maier, R.E. Savage, L.T. Haber, Assessing biomarker use in risk assessment—a survey of practitioners, J. Toxicol. Environ. Health 67 (2004) 687–695.
[3] E.A. Cohen Hubal, A.M. Richard, I. Shah, J. Gallagher, R. Kavlock, J. Blancato, S.W. Edwards, Exposure science and the U.S. EPA national center for computational toxicology, J. Expo. Sci. Environ. Epidemiol. 20 (2010) 231–236.
[4] B.K. Weis, D. Balshaw, J.R. Barr, D. Brown, M. Ellisman, P. Lioy, G. Omenn, J.D. Potter, M.T. Smith, L. Sohn, W.A. Suk, S. Sumner, J. Swenberg, D.R. Walt, S. Watkins, C. Thompson, S.H. Wilson, Personalized exposure assessment: promising approaches for human environmental health research, Environ. Health Perspect. 113 (2005) 840–848.
[5] G. Leng, W. Gries, New specific and sensitive biomonitoring methods for chemicals of emerging health relevance, Int. J. Hyg. Environ. Health 220 (2017) 113–122.
[6] C. Menale, D.G. Mita, N. Diano, S. Diano, Adverse Effects of Bisphenol A Exposure on Glucose Metabolism Regulation, Open Biotechnol. J. 10 (2016) 122–130.
[7] C. Menale, A. Grandone, C. Nicolucci, G. Cirillo, S. Crispi, A. Di Sessa, S. Rossi, D.G. Mita, L. Perrone, N. Diano, E. Miraglia Del Giudice, Bisphenol A is associated with insulin resistance and modulates adipokines gene expression in obese children, Pediatr. Obes. 12 (2017) 380–387.
[8] M. Dallio, M. Masarone, S. Errico, A.G. Gravina, C. Nicolucci, R. Di Sarno, L. Gionti, C. Tuccillo, M. Persico, P. Stiuso, N. Diano, C. Loguercio, A. Federico, Role of bisphenol A as environmental factor in the promotion of non-alcoholic fatty liver disease: in vitro and in vivo clinical study, Aliment. Pharmacol. Ther. 47 (2018) 826–837.
[9] Y. Zhu, Y. Cai, L. Xu, L. Zheng, L. Wang, B. Qi, C. Xu, Building An Aptamer/Graphene Oxide FRET Biosensor for One-Step Detection of Bisphenol A, ACS Appl. Mater. Interfaces 7 (2015) 7492–7496.
[10] J. Feng, L. Xu, G. Cui, X. Wu, W. Ma, H. Kuang, C. Xu, Building SERS-active heteroassemblies for ultrasensitive Bisphenol A detection, Biosens. Bioelectron. 81 (2016) 138–142.
[11] A.G. Asimakopoulos, N.S. Thomaidis, M.A. Koupparis, Recent trends in biomonitoring of bisphenol A, 4-t-octylphenol, and 4-nonylphenol, Toxicol. Lett. 210 (2012) 141–154.
[12] S. Errico, C. Nicolucci, M. Migliaccio, V. Micale, D.G. Mita, N. Diano, Analysis and occurrence of some phenol endocrine disruptors in two marine sites of the northern coast of Sicily (Italy), Mar. Pollut. Bull. 120 (2017) 68–74.
[13] C. Nicolucci, S. Errico, A. Federico, M. Dallio, C. Loguercio, N. Diano, Human exposure to Bisphenol A and liver health status: Quantification of Urinary and Circulating levels by LC-MS/MS, J. Pharm. Biomed. Anal. 140 (2017) 105–112.
[14] M.J. Baker, J. Trevisan, P. Bassan, R. Bhargava, H.J. Butler, K.M. Dorling, P.R. Fielden, S.W. Fogarty, N.J. Fullwood, K.A. Heys, Using Fourier transform IR spectroscopy to analyze biological materials, Nat. Protoc. 9 (2014) 1771–1791.
[15] D. Sheng, F. Xu, Q. Yu, T. Fang, J. Xia, S. Li, W. Xin, A study of structural differences between liver cancer cells and normal liver cells using FTIR spectroscopy, J. Mol. Struct. 1099 (2015) 18–23.
[16] O. Carnevali, V. Notarstefano, I. Olivotto, M. Graziano, P. Gallo, I. Di Marco Pisciottano, L. Vaccari, A. Mandich, E. Giorgini, F. Maradonna, Dietary administration of EDC mixtures: A focus on fish lipidmetabolism, Aquat. Toxicol. 185 (2017) 95–104.
[17] R. Chianese, A. Viggiano, K. Urbanek, D. Cappetta, J. Troisi, M. Scafuro, M. Guida, G. Esposito, L.P. Ciuffreda, F. Rossi, L. Berrino, S. Fasano, R. Pierantoni, A. De Angelis, R. Meccariello, Chronic exposure to low dose of bisphenol A impacts on the first round of spermatogenesis via SIRT1 modulation, Sci. Rep. 13 (2018) 2961, http://dx.doi.org/10.1038/s41598-018-21076-8.
[18] F. Severcan, O. Bozkurt, R. Gurbanov, G. Gorgulu, FT-IR spectroscopy in diagnosis of diabetes in rat animal model, J. Biophoton. 3 (2010) 621–631.
[19] V. Ricciardi, M. Portaccio, S. Piccolella, L. Manti, S. Pacifico, M. Lepore, Study of SH-SY5Y cancer cell response to treatment with polyphenol extracts using FT-IR spectroscopy, Biosensors 7 (2017) 57, http://dx.doi.org/10.3390/bios7040057.
[20] FDA, Guidance for Industry: Bioanalytical Method Validation, http://www.fda.gov/downloads/drugs/guidancecomplianceregulatoryinformation/guidances/ucm368107.pdf (Accessed 10.1.2017).
[21] W. Völkel, T. Colnot, G.A. Csanady, J.G. Filser, W. Dekant, Metabolism and kinetics of bisphenol A in humans at low doses following oral administration, Chem. Res. Toxicol. 15 (2002) 1281–1287.
[22] M.K. Moon, M.J. Kim, I.K. Jung, Y.D. Koo, H.Y. Ann, K.J. Lee, S.H. Kim, Y.C. Yoon, B.J. Cho, K.S. Park, H.C. Jang, Y.J. Park, Bisphenol A impairs mitochondrial function in the liver at doses below the no observed adverse effect level, J. Korean Med. Sci. 27 (2012) 644–652.
[23] L.N. Vandenberg, M.V. Maffini, C. Sonnenschein, B.S. Rubin, A.M. Soto, Bisphenol A and the great divide: a review of controversies in the field of endocrine disruption, Endocr. Rev. 30 (2009) 75–95.
[24] F.S. Vom Saal, G.S. Prins, W.V. Welshons, Report of very low, real-world exposure to bisphenol A is unwarranted based on a lack of data and flawed assumptions, Toxicol. Sci. 125 (2012) 318–320.
[25] F. Le Naour, M.P. Bralet, D. Debois, C. Sandt, C. Guettier, P. Dumas, A. Brunelle, O. Laprévote, Chemical Imaging on Liver Steatosis Using Synchrotron Infrared and ToF-SIMS Microspectroscopies, PLoS One 4 (10) (2007) e7408, http://dx.doi.org/10.1371/journal.pone.0007408.
[26] C. Peng, F. Chiappini, S. Kaščáková, M. Danulot, C. Sandt, D. Samuel, P. Dumas, C. Guettier, F. Le Naour, Vibrational signatures to discriminate liver steatosis grades, Analyst 140 (2015) 1107–1118.
[27] A. Melin, A. Perromat, G. Deleris, Pharmacologic application of Fourier transform IR spectroscopy: in vivo toxicity of carbon tetrachloride on rat liver, Biopolymers (Biospectroscopy) 57 (2000) 160–168.
[28] J.D. Browning, J.D. Horton, Molecular mediators of hepatic steatosis and liver injury, J. Clin. Invest. 114 (2004) 147–152.
[29] G. Barraza-Garza, H. Castillo-Michel, L.A. de la Rosa, A. Martinez-Martinez, J.A. Pérez-León, M. Cotte, E. Alvarez-Parrilla, Infrared Spectroscopy as a Tool to Study the Antioxidant Activity of Polyphenolic Compounds in Isolated Rat Erytrocytes, Oxid. Med. Cell. Longev. (2016) 9245150, http://dx.doi.org/10.1155/2016/9245150.
[30] S. Paglialunga, C.A. Dehn, Clinical assessment of hepatic de novo lipogenesis in non-alcoholic fatty liver disease, Lipids Health Dis. 15 (2016) 159, http://dx.doi.org/10.1186/s12944-016-0321-5.